LMR Based Plastic Optical Fiber Sensor Utilizing ITO Thin Film: A Theoretical Evaluation

Yu-Cheng Lin*

Department of Electronic Engineering, Ming Chuan University

ABSTRACT

The design of POF sensor based on lossy-mode resonance (LMR) was studied. The structure of sensing device is based on a D-shaped plastic optical fiber (POF) with a deposited thin-film layer of Indium Tin Oxide (ITO). The influence of the thickness of POF, sensing length and ITO thickness on the sensitivity is evaluated theoretically. Both POF thickness and sensing length have similar effect on LMR transmission spectra with the decreasing rate of 12.5 dB/mm and 0.82 dB/mm, respectively. As the ITO thickness increases, the dip wavelength of the LMR transmission is shifted toward the longer wavelength side with the sensitivity of 3.68 nm/nm. The ITO thickness is the key parameter to adjust the LMR wavelength. In terms of sensitivity, the LMR sensor with 50 nm or 75 nm thick ITO and 200 μ m to 400 μ m thick POF holds high sensitivity.

Keywords: lossy-mode resonance, plastic optical fiber, sensor, ITO thin film

以氧化銦錫薄膜製作的損耗模態共振型塑膠光纖感測器: 理論評估

林鈺城*

銘傳大學電子工程學系

摘 要

本篇論文研究基於損耗模態共振(LMR)的塑膠光纖感測器的設計。此感測元件的結構是利用在 D 形塑膠光纖(POF)上沉積了氧化銦錫(ITO)薄膜層,我們以理論計算了 POF厚度、感測長度和 ITO 厚度對靈敏度的影響。POF厚度和感測長度對 LMR 透射光譜強度具有相似的影響;它們的下降率分別是 12.5 dB/mm 和 0.82 dB/mm。隨著 ITO 厚度的增加,LMR波長以大約 3.68 nm/nm 的增長速率向更長的波長深度移動,所以,ITO 厚度是調整 LMR 波長位置的關鍵參數。就靈敏度而言,厚度 50 nm 或 75 nm 的 ITO 和厚度 $200~\mu$ m 到 $400~\mu$ m 的 POF製成的 LMR 感測器具較高的靈敏度。

關鍵詞:損耗模態共振,塑膠光纖,感測器,氧化銦錫薄膜

文稿收件日期 106.11.8; 文稿修正後接受日期 107.5.4; *通訊作者 Manuscript received November 8, 2017; revised May 4, 2018; * Corresponding author

I. INTRODUCTION

Thin-film coating of optical waveguides with semiconductor or metallic materials has become a widely explored technique in the field of sensors. The most well-known phenomenon is surface plasmon resonance (SPR). In recent years, SPR sensors have been extensively studied because of many applications ranging from biomaterials inspection, chemical detection, and physical test etc.[1-5] The SPR phenomenon occurs when the real part of the thin-film permittivity is negative and higher in magnitude than both its own imaginary part and the real part of the permittivity of the sampling material. Another lossy-mode resonances (LMRs) explained as a coupling between dielectric waveguide modes and a lossy-mode (a guided mode with a complex effective index) of semiconductor-clad waveguide were demonstrated by Marciniack [6]. Due to a coupling between waveguide modes and a specific lossy-mode, these resonances named as guided mode resonances [7] or LMRs [8]. This phenomenon is not limited to semiconductor claddings but it can be also observed for dielectric claddings. In fact, LMRs occur when the real part of the cladding permittivity is positive and higher in magnitude than both its own imaginary part and the real part permittivity of sampling materials. The generation of LMR with absorbing thin-films was analyzed with electromagnetic theory [9, 10]. The LMRs modal as a function of wavelength for thin-film coated on cladding removed silica optical fibers has been presented [11, 12]. From the point of view of cost effective fabrication, in order to generate LMRs, many materials can be used with the only condition of having optical losses rather than using expensive noble metals, such as gold or silver. From another point of optical performances, LMRs can be generated for both TM (transverse magnetic) and TE (transverse electric) polarizations. Furthermore, careful choosing the material could approach the same spectral band for both the TM mode and TE mode of LMR. It will enhance the signal-tonoise ratio of LMR sensors. So, the utilization of an optical polarizer, such as the SPR devices need, can be avoided. This simplification encourages the development of LMR sensors where only a wide-band light source and an optical spectrometer are necessary to setup the measurement. Compared with prism based sensors, optical fiber LMR sensors are fundamentally simpler in construction, less costly, more portable and more convenient to use but for little lower sensibility. In addition, optical fiber sensors can make real time and online remote detection of the refractive index variation of the bulk medium owing to optical fiber network implemented and wavelength spectrum integration adopted. In general, the optical fiber employed is either a glass one or a plastic one. For low-cost sensing systems, plastic optical fibers (POFs) are especially advantageous due to their excellent flexibility, easy manipulation, great numerical aperture, large diameter, and the fact that plastic is able to withstand smaller bend radii than glass. Fiberoptic-based sensors and, in particular, those using POFs are now widely recognized to offer various important advantages over traditional methods of sensing [13-15]. Further, advantages of special interest are the suitability of POFs to operate in a multi-sensor scheme, to permit monitoring in situ or remotely, and to be employed under harsh conditions without significant sensor performance deterioration. To enhance the sensitivity to a certain physical parameter, the guiding properties of optical fiber have to be weakened. The side polishing method offers a simple implementation since the mechanical resistance of POF allows an easy removal of a portion of the cladding and core. In addition, side polished POF sensors have demonstrated the advantages of easy waveguide alignment, high recurrence, mechanical stability and simple fabrication process. The great potential of LMR based optical fiber sensor technology for the detection of chemical and biological substances has been receiving growing interest from the scientific community. Therefore in this work, we propose design considerations for POF based on LMR sensor to investigate optimization of sensitivity. As per our knowledge, no study has been published on combining advantages of LMR and POF.

II. THEORY

Meridional cross section of the ITO-coated POF LMR sensor is shown in Fig.1. In this configuration, light is launched into the POF and

it is collected at the other end of the POF. In the middle of the optical path, there is a region where the core is side-polished, named as Dshape POF, and coated with ITO. For generality, Fig.1 gives the three-layer configuration consisting of a D-shaped POF core with thickness d_1 and refractive index n_1 , an ITO cladding layer with thickness d2 and refractive index n₂, and the sample layer with refractive index n₃. In order to obtain the transmitted optical power in the structure, it is applied first the attenuated total reflection (ATR) method with a Kretschmann configuration [16]. This model could applied here to estimates the reflection at the ITO-POF interface with the assumption of a planar structure. Consequently, there are two cases considered: the TE and TM polarization of the incidence light.

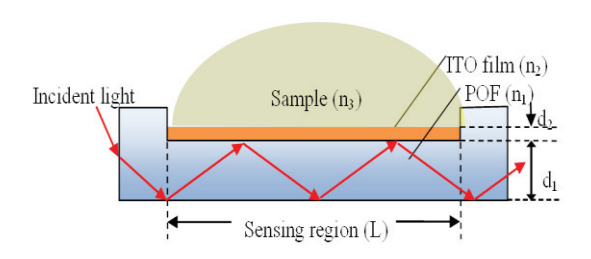


Fig. 1. three-layer configuration for LMR sensor

With this method the reflectivity $R(\theta, \lambda)$ as a function of wavelength and incidence angle is obtained at the ITO – POF core interface. Depending on the length of the film coated region and on the incidence angle, the number of reflections N at the ITO – POF core interface is obtained as

$$N(\theta) = \frac{L}{d_1 \tan \theta} \tag{1}$$

where L is the length of the film coated region and θ is the angle of incident light. The light from a wide band source is launched into one end of the POF. The power P arriving at another end of the POF as a function of incident angle θ is [17]

$$P(\theta, \lambda) \propto \left(\frac{2\pi}{\lambda}\right)^2 n_1^2 \cdot \sin\theta \cos\theta$$
 (2)

Using the reflectance value for a single reflection at the ITO/POF core interface, the transmission will be [17]

$$T(\lambda) = \frac{\int_{\theta cr}^{\pi/2} R^{N(\theta)} P(\theta, \lambda) d\theta}{\int_{\theta cr}^{\pi/2} P(\theta, \lambda) d\theta}$$
(3)

The θ_{cr} is the critical angle. Since the light introduced into the POF is unpolarized, $R^{N(\theta)}(\theta,\lambda)$ can be replaced with the reflectivity, a combination of TE and TM mode polarization. [17,18]

$$R^{N(\theta)}(\theta,\lambda) = \frac{1}{2} (R_{TE}^{N(\theta)} + R_{TM}^{N(\theta)})$$
 (4)

For TE components of $R^{N(\theta)}(\theta, \lambda)$ can be expressed as

$$R_{TE} = \frac{r_{12} + r_{23}e^{j2k_{2z}d_2}}{1 + r_{12}r_{23}e^{j2k_{2z}d_2}} \tag{5}$$

where
$$r_{12} = \frac{k_{1z} - k_{2z}}{k_{1z} + k_{2z}}$$
 (6)

$$r_{23} = \frac{k_{2z} - k_{3z}}{k_{2z} + k_{3z}} \tag{7}$$

$$k_{iz} = \sqrt{\left(\frac{2\pi}{\lambda}\right)^2 \epsilon_i - k_x^2} \quad i=1, 2, 3$$
 (8)

$$k_{x} = \frac{2\pi}{\lambda} n_{1} \sin \theta \tag{9}$$

The TM components of $R^{N(\theta)}(\theta, \lambda)$ can be expressed as

$$R_{TM} = \frac{r_{12} + r_{23}e^{j2k_{2z}d_2}}{1 + r_{12}r_{23}e^{j2k_{tz}d_2}} \tag{10}$$

$$r_{12} = \frac{\epsilon_2 k_{1z} - \epsilon_1 k_{2z}}{\epsilon_2 k_{1z} + \epsilon_1 k_{2z}} \tag{11}$$

$$r_{23} = \frac{\epsilon_3 k_{2z} - \epsilon_2 k_{3z}}{\epsilon_3 k_{2z} + \epsilon_2 k_{3z}} \tag{12}$$

Core of POF is assumed to be made of poly methyl methacrylate (PMMA). The refractive index of PMMA varies with wavelength according to Sellmeier dispersion relation [19] as

$$n_1(\lambda) = \sqrt{1 + \frac{a_1 \lambda^2}{\lambda^2 - b_1^2} + \frac{a_2 \lambda^2}{\lambda^2 - b_2^2} + \frac{a_3 \lambda^2}{\lambda^2 - b_3^2}}$$
 (13)

where, λ is the wavelength in μ m and a_1 , a_2 , a_3 , b_1 , b_2 and b_3 are Sellmeier coefficients and the values are given as, $a_1 = 0.99654$, $a_2 = 0.18964$, $a_3 = 0.00411$, $b_1 = 0.00787$ μ m, $b_2 = 0.02191$ μ m and $b_3 = 0.385727$ μ m, respectively.

Sensing layer is made of ITO. The most widely used expression for modeling ITO is the Drude model. Dielectric constant of ITO is written according to Drude model as [20].

$$\epsilon_2(\lambda) = 3.8 - \frac{\lambda_c \lambda^2}{\lambda_p^2 (\lambda_c + i\lambda)}$$

$$= 3.8 - \frac{\lambda_c^2}{\lambda_p^2} \frac{\lambda^2}{(\lambda^2 + \lambda_c^2)} + j \frac{\lambda_c}{\lambda_p^2} \frac{\lambda^3}{(\lambda^2 + \lambda_c^2)}$$

Here, λ_p and λ_c are the plasma wavelengths and the collision wavelength of ITO respectively, where $\lambda_p = 0.5649~\mu m$ and $\lambda_c = 11.121~\mu m$ for ITO [21]. According to the model of expression (14), the dispersion curves of index of refraction (real part) and extinction coefficient (imaginary part) are shown in Fig. 2. It can be seen that ITO is a hybrid material that behaves like a metal at longer wavelengths and a non-metallic nature at shorter wavelengths. Therefore, it satisfies both the conditions for LMRs generation at short wavelengths and the conditions for generation of SPRs at long wavelengths.

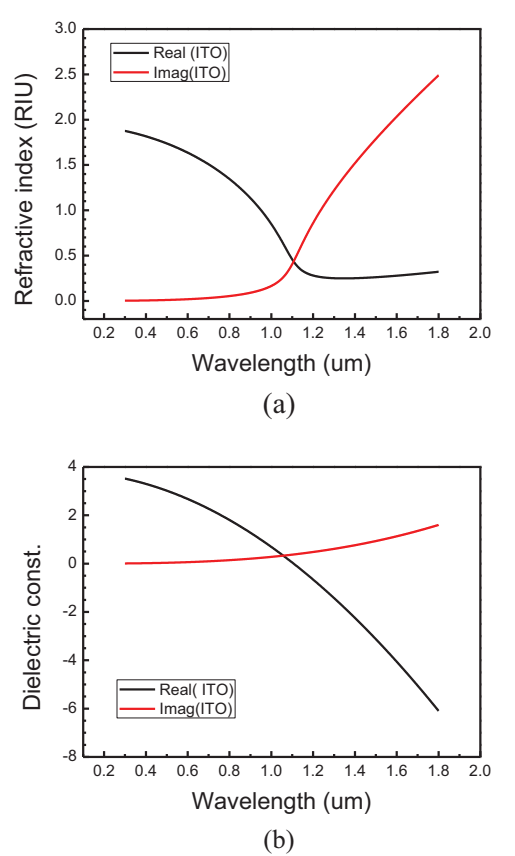


Fig.2. The Drude model simulation curves of ITO for (a) refractive index and (b) dielectric constant

III. RESULTS

the present study, for numerical calculations, the numerical aperture (NA) of POF is assumed to be 0.48 and the critical angle is about 72°. Fig.3(a) is a plot of the LMR POF sensor transmission spectra calculated with 200 μm, 400 μm, 600 μm and 800 μm exposed POF core thicknesses (d_1) . The theoretical results for LMR transmission spectrum are based on water sample $(n_3=1.33)$ obtained with the sensing length (L) 10 mm and the thickness of ITO (d_2) 0.1 µm. The transmitted spectral intensity distribution depends upon the core thickness of LMR sensing area. Thinner the POF core is, more reflection occurs during light propagating through the sensor and better LMR performance will be. So, the 200 µm thickness has a deeper transmission. The transmission deep and LMR wavelength shift versus POF thickness are shown in Fig.3(b). The POF thickness has obvious influence on transmission deep, at the decreasing rate of 12.5 dB/mm, rather than on LMR wavelength shift, the decreasing rate less than $3 \text{ nm}/100 \mu\text{m}$.

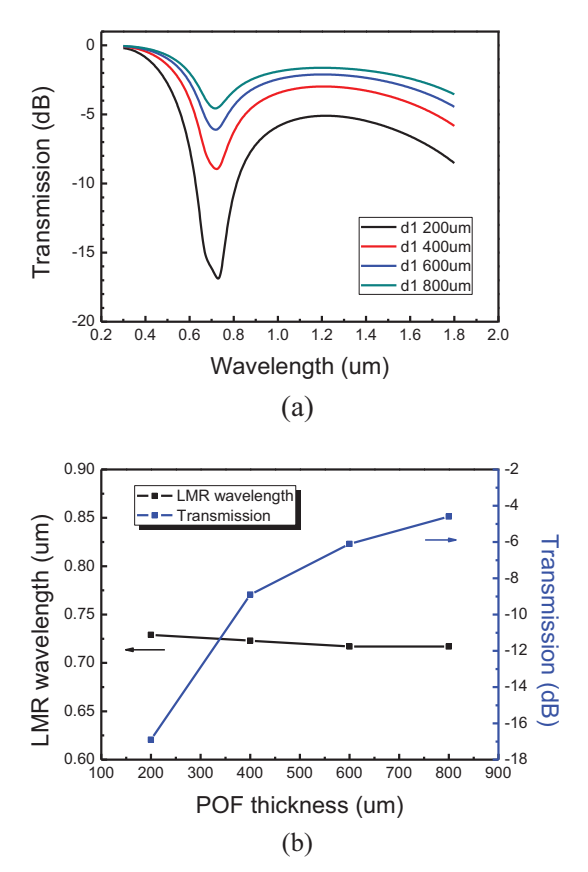


Fig.3 (a) Transmission curves of LMR POF sensor

with d_1 variation from 200 μ m to 800 μ m in step of 200 μ m; (b) the influence of d_1 on LMR wavelength and transmission deep

Fig.4(a) is a plot of the LMR POF sensor transmission spectra calculated for sensing length (*L*) varying from 5 mm to 20 mm in steps of 5 mm. The transmitted spectral-intensity distribution depends upon the length of LMR sensing area. The transmission deep and LMR wavelength shift versus sensing length is shown in Fig.4(b). As shown in Fig.4(b), the spectrum of a longer sensing area exhibits a deeper resonance and results in obvious transmission at the decreasing rate of 0.82 dB/mm. According to the eq.(1), both POF thickness (d₁) and sensing length have direct impact on the reflection times (*N*) and have similar big effect on LMR transmission spectra.

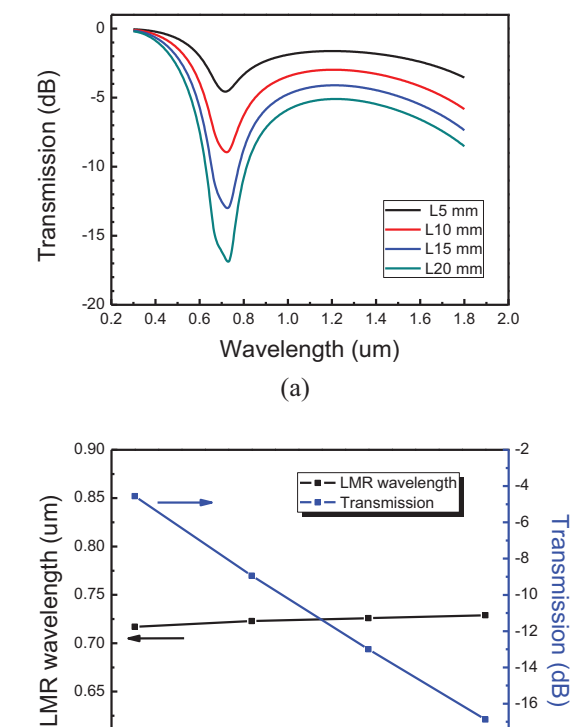


Fig.4 (a) Transmission curves of LMR POF sensor with sensing length L varying from 5 mm to 20 mm in steps of 5 mm; (b) the influence of L on LMR wavelength shift and transmission deep

(b)

LMR length (mm)

18

0.60

Fig.5(a) shows the theoretical results for typical LMR spectra of water obtained with the

sensors having different ITO thicknesses (d2) from 50 nm to 125 nm in step of 25 nm. The transmission and LMR wavelength shift versus ITO thickness is shown in Fig.5(b). As can be seen in Fig.5(b), there are spectra that show a large LMR wavelength shift. As the ITO thickness increases, the shift of the reflectance LMR spectrum toward longer wavelengths at the increasing rate about 3.68 nm/nm. In contrast, it has no obvious variation on LMR transmission deep. The LMR could not be excited when ITO thickness is thinner than 50 nm. On the other hand, when ITO is thicker than 125 nm, other LMR modes will appear. So, there are also other remarkable advantages of LMRs. Their spectral position can be fine-tuned just by changing the thickness of the lossy coating. Even more, instead of having a unique optical resonance, several resonances can appear when the thickness or the lossy coating is increased and all these peaks can be used for sensing or other applications.

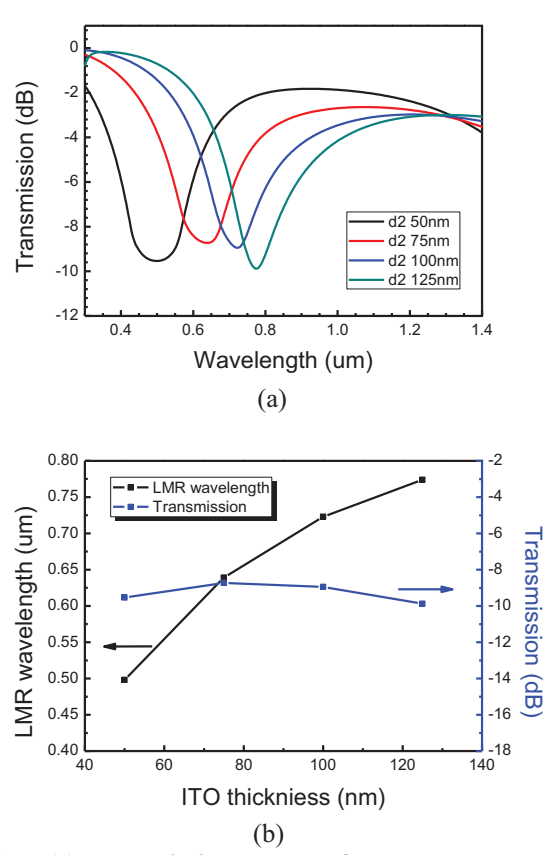


Fig.5 (a) Transmission curves of LMR POF sensor with ITO thickness d₂ varying from 50 nm to 125 nm in steps of 25 nm; (b) the influence of d₂ on LMR wavelength shift and transmission deep

If the refractive index of the sensing sample is altered by δn , the resonance wavelength shifts by $\delta \lambda_{res}$. The sensitivity (S_n) of an LMR sensor with spectral interrogation is defined as

$$S_n = \frac{\delta \lambda_{res}}{\delta n} \tag{15}$$

To calculate the sensitivity, $\delta \lambda_{res}$ is plotted as a function of d₂ variation from 25 nm to 125 nm in steps of 25 nm for different ITO thickness (d₂) 200 μm, 400 μm and 600 μm, shown in Fig.6. The higher sensitivities for d₁ of 200 µm, 400 μm and 600μm are 1140 nm/RIU at d₂ 50 nm, 1040 nm/RIU at d₂ 50 nm and 840 nm/RIU at d₂ 75 nm, respectively. Thus in terms of above discussions, it is concluded that d₁ 200 µm and d₂ 50 nm based LMR sensor displays good sensing behavior and approaches high sensitivity 1140 nm/RIU. Besides it, Fig. 7 reveals the LMR transmission curves for 200 µm thick POF and 50 nm thick ITO layer based sensor for refractive of sensing medium from 1.33 to 1.39 in steps of 0.02. All the transmission deeps are lower than -10dB. The LMR wavelength varies from 660 nm to 714 nm.

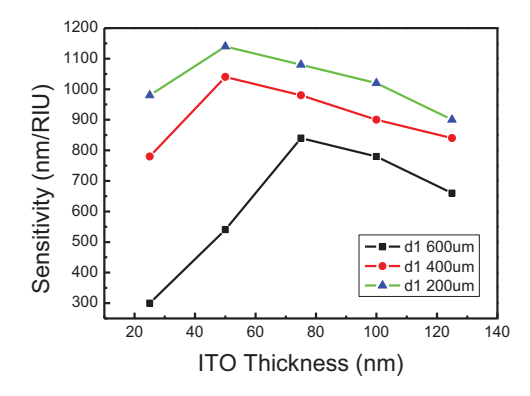


Fig.6. Sensitivity is plotted as a function of d_2 variation from 25 nm to 125 nm in steps of 25 nm for different ITO thickness (d_1) 200 μ m, 400 μ m and 600 μ m

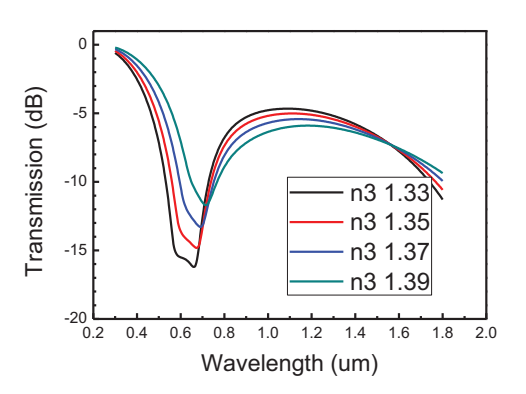


Fig. 7. The LMR transmission curves for 200 µm thick POF and 50 nm thick ITO layer based POF sensor for refractive of sensing medium from 1.33 to 1.39 in steps of 0.02

VI. CONCLUSIONS

We proposed a LMR based POF sensor with a ITO thin film coated and the structure parameters are theoretically inspected. The POF thickness and the LMR sensing length have large influence on transmission deep; however, they have little effect on the LMR wavelength shift. The ITO thickness is the key parameter to adjust the LMR wavelength. In terms of sensitivity, the results show that the LMR sensor with 50 nm to 75 nm thick ITO and 200 μm to 400 μm thick POF holds high sensitivity.

ACKNOWLEDGEMENTS

The authors would like to thank the Ministry of Science and Technology for financial support under the contracts MOST 106-2221-E-130-011.

REFERENCES

- [1] R. Verma and B. D. Gupta, "Detection of heavy metal ions in contaminated water by surface plasmon resonance based optical fibre sensor using conducting polymer and chitosan," Food Chemistry, vol. 166, pp. 568-575, 2015.
- [2] S. Qian, Y. Liang, J. Ma, Y. Zhang, J. Zhao, and W. Peng, "Boronic acid modified fiber optic SPR sensor and its application in saccharide detection," Sensors and

- Actuators B: Chemical, vol. 220, pp. 1217-1223, 2015.
- [3] K. Shah, N. K. Sharma, and V. Sajal, "SPR based fiber optic sensor with bi layers of indium tin oxide and platinum: A theoretical evaluation," Optik International Journal for Light and Electron Optics, vol. 135, pp. 50-56, 2017.
- [4] N. Cennamo, M. Pesavento, L. Lunelli, L. Vanzetti, C. Pederzolli, L. Zeni, et al., "An easy way to realize SPR aptasensor: A multimode plastic optical fiber platform for cancer biomarkers detection," Talanta, vol. 140, pp. 88-95, 2015.
- [5] R. Verma and B. D. Gupta, "Fiber optic SPR sensor for the detection of 3pyridinecarboxamide (vitamin B-3) using molecularly imprinted hydrogel," Sensors and Actuators B-Chemical, vol. 177, pp. 279-285, 2013.
- [6] M. Marciniak, J. Grzegorzewski, and M. Szustakowski, "Analysis of lossy mode cut-off conditions in planar waveguides with semiconductor guiding layer," IEE Proceedings J-Optoelectronics, vol. 140, pp. 247-252, 1993.
- [7] H. R. E. Kretchmann, "Radiative decay of non-radiative surface plasmons excited by light," Z. Naturforsch, vol. 23, pp. 2135-2136, 1968.
- [8] R. Verma and B. D. Gupta, "Optical fiber sensor for the detection of tetracycline using surface plasmon resonance and molecular imprinting," Analyst, vol. 138, pp. 7254-7263, 2013.
- [9] F. J. Arregui, I. Del Villar, J. M. Corres, J. Goicoechea, C. R. Zamarreño, C. Elosua, et al., "Fiber-optic Lossy Mode Resonance Sensors," Procedia Engineering, vol. 87, pp. 3-8, 2014.
- [10] I. D. Villar, C. R. Zamarreno, M. Hernaez, F. J. Arregui, and I. R. Matias, "Lossy Mode Resonance Generation With Indium-Tin-Oxide-Coated Optical Fibers for Sensing Applications," Journal of Lightwave Technology, vol. 28, pp. 111-117, 2010.
- [11] M. Hernáez, I. Del Villar, C. R. Zamarreño, F. J. Arregui, and I. R. Matias, "Optical fiber refractometers based on lossy mode resonances supported by TiO 2 coatings," Applied optics, vol. 49, pp. 3980-3985,

- 2010.
- [12] A. B. Socorro, J. M. Corres, I. Del Villar, F. J. Arregui, and I. R. Matias, "Fiber-optic biosensor based on lossy mode resonances," Sensors and Actuators B: Chemical, vol. 174, pp. 263-269, 2012.
- [13] J. Shin and J. Park, "Plastic Optical Fiber Refractive Index Sensor Employing an In-Line Submillimeter Hole," IEEE Photonics Technology Letters, vol.25, no.19, pp. 1882 – 1884, 2013.
- [14] H. Saad, M. K. A. Rahman, and M. T. Ali, "Tapered plastic optical fiber sensor for detection of ethanol concentration in H2O," in Sensing Technology (ICST), 2013 Seventh International Conference on, 2013, pp. 559-564.
- [15] P. Aiestaran, J. Arrue, and J. Zubia, "Design of a sensor based on plastic optical fibre (POF) to measure fluid flow and turbidity," Sensors, vol. 9, pp. 3790-3800, 2009.
- [16] J. Homola and M. Piliarik, "Surface Plasmon Resonance (SPR) Sensors," in Surface Plasmon Resonance Based Sensors, J. Homola, Ed., ed Berlin, Heidelberg: Springer Berlin Heidelberg, 2006, pp. 45-67.
- [17] Y. Xu, N. B. Jones, J. C. Fothergill, and C. D. Hanning, "Analytical estimates of the characteristics of surface plasmon resonance fibre-optic sensors," Journal of Modern Optics, vol. 47, pp. 1099-1110, 2000.
- [18] A. K. Sharma and B. D. Gupta, "On the sensitivity and signal to noise ratio of a step-index fiber optic surface plasmon resonance sensor with bimetallic layers," Optics Communications, vol. 245, pp. 159-169, 2005.
- [19] S. N. Kasarova, N. G. Sultanova, C. D. Ivanov, and I. D. Nikolov, "Analysis of the dispersion of optical plastic materials," Optical Materials, vol. 29, pp. 1481-1490, 2007.
- [20] S. K. Srivastava, R. Verma, and B. D. Gupta, "Theoretical modeling of a self-referenced dual mode SPR sensor utilizing indium tin oxide film," Optics Communications, vol. 369, pp. 131-137, 2016.
- [21] C. Rhodes, M. Cerruti, A. Efremenko, M.

Losego, D. E. Aspnes, J.-P. Maria, et al., "Dependence of plasmon polaritons on the thickness of indium tin oxide thin films," Journal of Applied Physics, vol. 103, p. 093-108, 2008.Bobrow, J. E., "A direct minimization approach for obtaining the distance between convex polyhedral," International Journal of Robotics Research, Vol. 8, No. 3, pp. 65-76, 1989.